Environmental Science
Processes & Impacts

Exploring Matrix Effects and Quantifying Organic Additives in Hydraulic Fracturing Associated Fluids Using Liquid Chromatography Electrospray Ionization Mass Spectrometry

SCHOLARONE™
Manuscripts

1 **TITLE:** Exploring Matrix Effects and Quantifying Organic Additives in Hydraulic Fracturing Associated

2 Fluids Using Liquid Chromatography Electrospray Ionization Mass Spectrometry

3

4 **AUTHORS:** Marika Nell and Damian E. Helbling

5

6 **AFFILIATION:** School of Civil and Environmental Engineering, Cornell University, Ithaca, NY, USA

7

8 **CORRESPONDING AUTHOR:** Damian E. Helbling, School of Civil and Environmental Engineering, Cornell

9 University, 220 Hollister Hall, Ithaca, NY, 14853, USA. Email: damian.helbling@cornell.edu. Tel: +1 607

10 255 5146. Fax: +1 607 255 9004.

11

12 **Environmental Significance Statement:** The complex matrix of hydraulic fracturing (HF) associated fluids

13 has limited the applicability of electrospray ionization-based analytical techniques for quantitative

14 analysis of polar to semi-polar chemical additives. Improved understanding of the concentrations of

15 various analytes in HF associated fluids is an essential prerequisite to evaluate wastewater disposal

16 strategies or assess the environmental risk of contamination events or spills. We systematically

17 evaluated matrix recovery factors for seventeen priority HF additives and applied them to provide the

18 first known quantification of several HF additives in HF associated fluids. Our approach allows us to

19 overcome the uncertainties associated with complex matrices and can be generalized to other

20 wastewater samples across wells and shale formations.

ABSTRACT

22 Hydraulic fracturing (HF) operations utilize millions of gallons of water amended with chemical additives

23 including biocides, corrosion inhibitors, and surfactants. Fluids injected into the subsurface return to the

24 surface as wastewaters, which contain a complex mixture of additives, transformation products, and

25 geogenic chemical constituents. Quantitative analytical methods are needed to evaluate wastewater

26 disposal alternatives or to conduct adequate exposure assessments. However, our narrow

27 understanding of how matrix effects change the ionization efficiency of target analytes limits the

28 quantitative analysis of polar to semi-polar HF additives by means of liquid chromatography electrospray

29 ionization mass spectrometry (LC-ESI-MS). To address this limitation, we explored the ways in which

30 matrix chemistry influences the ionization of seventeen priority HF additives with a modified standard

31 addition approach. We then used the data to quantify HF additives in HF-associated fluids. Our results

32 demonstrate that HF additives generally exhibit suppressed ionization in HF-associated fluids, though HF

33 additives that predominantly form sodiated adducts exhibit significantly enhanced ionization in

34 produced water samples, which is largely the result of adduct shifting. In a preliminary screening, we

35 identified glutaraldehyde and 2-butoxyethanol along with homologues of benzalkonium chloride

36 (ADBAC), polyethylene glycol (PEG), and polypropylene glycol (PPG) in HF-associated fluids. We then

37 used matrix recovery factors to provide the first quantitative measurements of individual homologues of

38 ADBAC, PEG, and PPG in HF-affiliated fluids ranging from mg·L^{-1} levels in hydraulic fracturing fluid to low

39 μg·L^{-1} levels in PW samples. Our approach is generalizable across sample types and shale formations and

40 yields important data to evaluate wastewater disposal alternatives or implement exposure assessments.

41 **INTRODUCTION**

42   The use of hydraulic fracturing (HF), coupled with horizontal drilling, has led to a boom in

43 unconventional shale gas production over the course of the past decade. For example, as the United

44 States (US) sought to become a natural gas exporter, hydraulic fracturing played a critical role—already

45 in 2015, hydraulically fractured wells accounted for 67% of all US natural gas production.[1,2] However,

46 concerns about the environmental and human health impacts of HF remain.[3,4] In the HF process,

47 hydraulic fracturing fluid (HFF), which is a mix of makeup water (MW – i.e., surface water, groundwater,

48 or recycled wastewater),[5] a proppant, and up to two percent chemical additives, is injected into a well at

49 high pressure and temperature to increase the permeability of the target formation. When pressure is

50 released from the well, a mix of geogenic brine and HFF returns to the surface as flowback water (FW).

51 Over time, this wastewater will continue to flow from the well as produced water (PW) and its matrix

52 will more closely resemble the geogenic brine sourced from the formation porewater, although there is

53 no clearly defined point at which FW turns to PW.[6,7] While relatively few HF additives are used to

54 fracture any single well, over one thousand HF additives have been disclosed including biocides,

55 corrosion inhibitors, and surfactants.[7] A review of these additives found that up to 37% could have

56 endocrine disrupting effects and 25% could have mutagenic or carcinogenic affects, highlighting the

57 need for both toxicological studies and the ability to determine the level of exposure in the event of

58 environmental contamination.[8] Because contamination can occur at any point in the HF process, it is

59 critical to establish quantitative analytical methods that detect a broad range of contaminants of

60 concern in all HF-associated fluids including MW, HFF, FW, and PW.

61   To date, most analytical methods developed and applied to characterize the organic

62 composition of HF-associated fluids have utilized gas chromatography mass spectrometry (GC-MS) to

63 quantify hydrophobic organic constituents that are less likely to be persistent and mobile in

64 groundwater or surface water.[9–11] Very few studies have focused on quantification of polar to semi-polar

65   HF additives and their transformation products that are likely to be more relevant for water quality.

66   Liquid chromatography electrospray ionization mass spectrometry (LC-ESI-MS) offers sensitive and

67   accurate analysis of polar to semi-polar analytes in water samples and is expected to play an important

68   role in improving our understanding of the chemistry of HF-associated fluids. A few studies have used

69   LC-ESI-MS to detect semi-polar to polar additives in HF wastewater samples,[12–17] though all have been

70   qualitative or semi-quantitative in nature. This limits our ability to extrapolate the data for toxicity

71   studies or exposure assessments.

72   One major limitation of applying existing LC-ESI-MS methods for the quantification of HF

73   additives in environmental samples is the complex and changing matrix of HF-associated fluids, which

74   can lead to complicating matrix effects in ESI-based analyses.[16,18] Matrix effects can lead to enhanced or

75   suppressed ionization of target analytes, and there are at least two important ways in which matrix

76   effects can limit chemical analyses in HF-associated fluids. First, inorganic or organic matrix constituents

77   that co-elute with target analytes may enhance or suppress the ionization of the target analytes. For

78   example, surfactants can dominate the surface of droplets formed in the ESI source, enhancing their

79   ionization and detection, but suppressing the ionization of other co-eluting analytes.[19–21] Second,

80   complex matrix chemistry can affect the ways in which a target analyte is ionized, including the types of

81   adducts which may be formed during ESI. For example, an analyte that predominantly forms protonated

82   adducts $[M+H]^+$ during ESI when present in a clean water matrix may form a disproportionate amount of

83   sodiated adducts $[M+Na]^+$ during ESI when present in saline FW or PW samples.[13] Sodiated adducts pose

84   a problem for typical methods of quantification because they do not fragment as well as protonated

85   adducts.[15]

86   Matrix effects have confounded environmental analytical chemistry for decades and a variety of

87   techniques have been developed to account for matrix effects in LC-ESI-MS analyses.[19,22–24] The most

88   widely used technique is the addition of isotope labeled internal standards (ILISs).[25] If an ILIS can be

4

89   acquired or synthesized for each target analyte, then any matrix effect experienced by the analyte will

90   also be experienced by the ILIS and appropriate corrections can be made during quantification.

91   Unfortunately, very few ILISs are available for polar to semi-polar HF additives. Another approach is to

92   prepare matrix-matched calibration curves.[26,27] Whereas this is an appropriate and effective technique,

93   it is generally only applied across samples with uniform matrices and may require additional preparation

94   to create a matrix blank that does not contain any of the target analytes.[28] The matrix of FW and PW

95   varies from well to well and evolves over time, making preparation of matrix-matched calibration curves

96   impractical and cost-prohibitive.[6,29,30] Finally, standard addition and the calculation of matrix recovery

97   factors (MRFs) have been used to quantify analytes by relating responses obtained in, for example,

98   calibration curves measured in one matrix to responses obtained in samples with a more complex

99   matrix.[16,22,23,31] MRFs calculated for a given analyte in a particular matrix have the added benefit of

100   providing a metric by which the mechanisms of enhanced or suppressed ionization efficiency can be

101   carefully examined.

102   The objectives of this study were to (i) evaluate the LC-ESI-MS acquisition parameters for a

103   diverse set of polar and semi-polar HF additives, (ii) explore how matrix chemistry influences the

104   ionization behavior of each of the additives through a modified standard addition approach, (iii) screen

105   for the occurrence of HF additives in MW, HFF, FW, and PW samples, and (iv) apply MRFs to quantify the

106   HF additives in the MW, HFF, FW, and PW samples. We collected field samples from two unconventional

107   shale gas wells in Morgantown, WV. Our approach elucidates the ways in which matrix chemistry

108   influences the ionization behavior of certain types of HF additives and enables the first known

109   quantification of several priority HF additives in field samples by means of LC-ESI-MS.

110   **METHODS**

111   **Standards and Reagents.** We selected nineteen HF additives or likely transformation products based on

112   their amenability to LC-ESI-MS analysis,[12] their identification as additives of concern,[4,32] or their inclusion

113   in the FracFocus chemical disclosure for the sampling location. Compound names, compound uses, CAS

114   numbers, and chemical structures are provided in Table ESI1 of the Electronic Supplementary

115   Information (ESI). We acquired twelve of the HFF additives as individual compounds of varying purity

116   and seven as homologous mixtures containing varying numbers of individual homologues (*e.g.*,

117   polyethylene glycol, PEG). See Tables ESI2 and ESI3 for details on suppliers and purities of individual

118   compounds and homologous mixtures, respectively. We prepared stock solutions of each individual

119   compound or homologous mixture at a concentration of 1 $g \cdot L^{-1}$ in LC-MS grade methanol (Omnisolv,

120   VWR) or nanopure water (produced by a Milli-Q system, EMD Millipore). We then used these stock

121   solutions to prepare standard solutions and mixtures of all HFF additives in nanopure water at 1 $mg \cdot L^{-1}$

122   and 100 $\mu g \cdot L^{-1}$. We stored all standard solutions and mixtures at −20 °C.

123   **Compound Tuning.** We optimized MS acquisition parameters for each individual HFF additive by direct

124   infusion into a quadrupole-Orbitrap mass spectrometer (QExactive, ThermoFisher Scientific). We used a

125   syringe pump to deliver 20 to 50 $\mu L \cdot min^{-1}$ of each standard solution ranging from 100 $\mu g \cdot L^{-1}$ to 10 mg/L

126   to a tee connection receiving 50 $\mu L \cdot min^{-1}$ to 200 $\mu L \cdot min^{-1}$ of mobile phase (90% LC-MS grade water and

127   10% LC-MS grade methanol, both augmented with 0.1% formic acid by volume) and connected directly

128   to the ESI source. We identified the optimal polarity and the exact mass of the dominant ion or adduct

129   (e.g., $[M+H]^+$, $[M+Na]^+$, etc.) in full scan MS acquisitions in positive and negative polarity modes. We

130   identified the optimal collision energy for MS/MS fragmentation and the exact masses of the dominant

131   MS/MS fragments for each additive under a range of normalized collision energies (NCEs). We defined

132   the optimal collision energy as the value that resulted in the highest total intensity of unique MS/MS

133   fragments. Identifying optimal collision energies for homologous mixtures required chromatographic

134   separation. We acquired these values using the LC-ESI-MS gradient method described below and

135   acquired MS/MS data using NCE values ranging from 15 to 90.

136   **Sample Collection.** In collaboration with the West Virginia Water Research Institute and the Marcellus

137   Shale Energy and Environment Laboratory (MSEEL), we collected fourteen water samples from two

138   unconventional shale gas wells in Morgantown, WV. The wells are known as MIP 5H and MIP 3H[33] and

139   both are horizontal wells drilled from the same pad. MIP 5H was hydraulically fractured on 11/6/15 and

140   MIP 3H was hydraulically fractured on 11/9/15. We collected seven water samples related to each well,

141   including a sample of the MW and HFF from the day the well was completed, a sample of FW from the

142   day pressure was released from the well, and four weekly samples of PW from the first month that the

143   wells were producing. The MW was sourced from the Monongahela River, although any water that was

144   stored from drilling may have been mixed with the Monongahela River water. We collected all samples

145   in 1 L TraceClean amber glass bottles (VWR). A complete listing of samples, sample dates, and

146   corresponding sample metadata can be found in Table ESI4. We stored the samples at 4°C for up to one

147   month before they were shipped to our laboratory, where we then stored them at -20°C until analysis.

148   **Sample Preparation.** Prior to all experiments and analyses by LC-ESI-MS, we thawed raw samples,

149   adjusted their pH to 9.8-10 using ammonia, filtered them with 0.45 µm PTFE filters[13] (Restek), adjusted

150   them to neutral pH using formic acid, and diluted them using nanopure water. Adjustments to pH and

151   filtration were required to remove particles and precipitates that interfere with LC separations. Dilution

152   was required to reduce the intensities of mass spectral features. MW, FW, and PW were diluted by a

153   factor of 10. HFF was diluted by a factor of 100 for matrix recovery experiments and a factor of 1000 for

154   quantification of benzalkonium chloride (ADBAC).

155   **Matrix Recovery Experiment.** To explore the ways in which the water sample matrices influence the

156   ionization of the HFF additives relative to their ionization in nanopure water, we spiked a mixture of the

157   nineteen selected HFF additives into each of the fourteen prepared water samples and nanopure at

158   varying concentrations. We selected concentrations so that the resulting chromatographic peaks would

159   have an intensity between 1E7 and 7E7 in nanopure water, ensuring that the compound would be

160   detected in the prepared water samples even if its ionization was suppressed by 90% and would not

161   overfill the mass detector if its ionization was enhanced. It must be noted that we selected the spiked

162   concentration in this way to enable robust estimation of MRFs, though this approach may limit the

163   application of MRFs for quantification if the concentration of the additive in the sample is significantly

164   different than the spiked concentration. The selected concentration for each of the HFF additives is

165   provided in Table ESI5. We measured each of the prepared and spiked water samples by means of LC-

166   ESI-MS and calculated MRFs according to Equation 1:

$$Matrix\ Recovery\ Factor\ (MRF) = \frac{Peak\ Area_{Spiked\ Samples} - Peak\ Area_{Samples}}{Peak\ Area_{Spiked\ Nanopure} - Peak\ Area_{Nanopure}}$$ Equation 1

167   We conducted matrix recovery experiments in triplicate and we report all MRFs as the average of three

168   measurements.

169   **Analytical HPLC-ESI-MS Method.** We measured standard solutions, standard mixtures, prepared water

170   samples, and spiked water samples by means of high-performance liquid chromatography (HPLC)

171   electrospray ionization (ESI) quadrupole-Orbitrap mass spectrometry (MS) (QExactive, ThermoFisher

172   Scientific) using an analytical method that we adapted from previous work focusing on the broad

173   detection of organic micropollutants (log K_{ow} -3 to +6) in water samples.[34,35] Briefly, the analytical

174   method incorporated large-volume injection to retain polar and semi-polar compounds on a C18 trap

175   column (Hypersil Gold aQ, 2.1x20 mm, 12 µm particle size, ThermoFisher Scientific) while diverting the

176   majority of inorganic matrix constituents to waste. Samples were then eluted from the trap column and

177   onto a C18 analytical column (XBridge, 2.1 x 50 mm, 3.5 µm particle size, Waters) for chromatographic

178   separation. Details on the mobile phase composition and gradient programs are provided in Tables ESI6

179   and ESI7 and elsewhere.[34,35] We performed MS analysis in rapid polarity switching mode to include

180   positive and negative ESI in the same run. Details of MS and MS/MS acquisition parameters are provided

181   in Table ESI8. For quantification of HFF additives, we created a six-point calibration curve by diluting the

182   standard mixture with nanopure water. To explore methods for quantification of individual homologues

183   present in a homologous mixture, we created separate six-point calibration curves with a pure standard

184   of benzyldimethyldodecyl ammonium (ADBAC-C_{12}) and a homologous mixture containing ADBAC-C_{12},

185   ADBAC-C_{14} and ADBAC-C_{16}. Finally, we determined retention times (RTs) and limits of detection (LODs)

186   for each of the HFF additives included in the standard mixture by inspection of the calibration curves as

187   described in the ESI. Screening for HF additives in water samples was done by matching RTs, accurate

188   masses, and MS/MS fragments with the standards of individual the compounds as previously

189   described.[35]

190   **Statistical Analyses.** We used Microsoft Excel 2016 to conduct one-way ANOVA tests to compare MRFs

191   among individual homologues in homologous series. We used IBM SPSS Statistics (Version 25) to

192   conduct a Friedman test followed by pairwise comparisons with a Bonferroni correction for multiple

193   comparisons to assess differences in the mean MRFs across water samples. All statistical tests used an

194   alpha value of 0.05 to evaluate significance.

195   **RESULTS & DISCUSSION**

196   **Analytical Response to HFF Additives.** The optimized MS and MS/MS acquisition parameters for each of

197   the nineteen HF additives measured in nanopure water during compound tuning is provided in Table

198   ESI9; representative homologues are described for HF additives acquired as homologous mixtures.

199   Eighteen of the HF additives ionized more efficiently in positive polarity mode, with 2-acrylamido-2-

200   methylpropanesulfonic acid being the only individual compound that ionized more efficiently in negative

201   polarity mode. We noted a number of ions and adducts during compound tuning including protonated

202   adducts $[M+H]^+$, deprotonated compounds $[M-H]^-$, sodiated adducts $[M+Na]^+$, ammoniated adducts

203    $[M+NH_4]^+$, adducts of methanol $[M+CH_3OH+H]^+$, and adducts incorporating various conjugates of the HF

204   additives. The three quaternary ammonium compounds (ADBAC, cocamidopropyl hydroxysultaine

205   (CAPHS), and didecyldimethylammonium chloride) carry positive charges and were measured as $[M]^+$.

206   RTs and LODs acquired from the analysis of calibration curves are also provided in Table ESI9. The

207   analytical method simultaneously detects seventeen of the nineteen HFF additives with adequate

208   chromatographic resolution and LODs, with the exceptions being ethylenediaminetetraacetic acid

209   (EDTA) and bis(hexamethylene) triamine which were not detected with our analytical method when

210   spiked into the HF fluids. The LODs for each of the HF additives in nanopure water range between 50

211    $ng \cdot L^{-1}$ to 50 $\mu g \cdot L^{-1}$ which is more sensitive than previously reported analytical methods for ADBAC,

212   glutaraldehyde, and cocoamidopropyl surfactants[13], likely due to our use of large-volume injection.

213   **Calculation of Matrix Recovery Factors.** The matrix chemistry of HFF wastewaters is complex.[6,29,36] The

214   TDS and inorganic cation concentrations measured in each of the fourteen water samples from MIP 3H

215   and 5H are provided in Table ESI4 and Figure ESI1, respectively. Of note among these data are increases

216   in TDS concentrations in FW and PW samples (from ppm levels in MW and HFF to parts per thousand

217   levels in FW and PW) and the concomitant increase in the concentrations of inorganic cations in those

218   water samples, particularly of sodium and calcium cations. Additionally, changes in total organic carbon

219   concentrations resulting from natural organic matter (NOM) and the presence of surfactants and other

220   HF additives have been routinely reported in HFF wastewaters.[29,37] We expect these changes in matrix

221   chemistry to alter the ionization behavior of HF additives in a number of possible ways, though we have

222   insufficient knowledge to predict how these complex changes in matrix chemistry will alter the

223   ionization behavior of HF additives. Therefore, we calculated MRFs for each of the seventeen detected

224   HF additives by spiking a mixture of each additive into each of the prepared water samples collected

225   from MIP 3H and 5H. MRFs describe the ways in which the water sample matrices influence the

226   ionization of the HF additives relative to their ionization in nanopure water. MRFs greater than 1.0

227   indicate enhanced ionization in a matrix relative to nanopure and MRFs less than 1.0 indicate

228   suppressed ionization in a matrix relative to nanopure.

229   We hypothesized that the overall magnitude of the MRFs will vary for compounds that ionize in

230   different ways (e.g., those that form different types of adducts) and among water samples. To test this

Environmental Science: Processes & Impacts

231   hypothesis, we calculated MRFs for each additive and in each water sample and present a portion of

232   these data in **Figure 1** (the full dataset is provided in Table ESI10). We present the average of triplicate

233   MRFs for all individual compounds and a representative homologue for each homologous mixture that

234   generated nonzero MRFs and were either positively charged, deprotonated, or formed protonated or

235   sodiated adducts. Average MRFs greater than 1.0 are shown with shades of blue and average MRFs less

236   than 1.0 are shown with shades of red. The coefficient of variation of all MRFs was typically less than

237   15%, indicating that our estimates of average MRFs are relatively robust in most instances.

238   The data in **Figure 1** provide important insights on the behavior of each additive in each type of

239   water sample. First, it is clear that most of the additives exhibit suppressed ionization in most types of

240   water samples. This is consistent with the expectations for a complex matrix, where interfering organic

241   compounds may co-elute with target analytes.[38,39] Second, we expected that the quaternary ammonium

242   compounds $[M]^+$ would not exhibit significant signal suppression because surfactants dominate the

243   surface of droplets formed during ESI[21] and would not experience adduct shifting because their

244   ionization is independent of the matrix or other water chemistry parameters. Therefore, it is notable

245   that the ionization behavior of ADBAC-C_{12} is rather stable across all matrix types, whereas the ionization

246   of CAPHS-C_7H_{15} and didecyldimethylammonium is generally suppressed across all matrix types. Further,

247   ADBAC-C_{12} and CAPHS-C_7H_{15} have similar RTs (18.0 and 18.2, respectively) which we expected would

248   contribute to similar changes in ionization behavior if the effects were due to co-elution. These

249   observations complicate our interpretation of these data and suggest that the ionization cannot be

250   generalized from one cationic compound to another, which limits our ability to predict the behavior of

251   untested cationic compounds. Finally, the additives that favor protonated adducts $[M+H]^+$ or are

252   deprotonated $[M-H]^-$ in nanopure exhibit limited matrix effects in MW and HFF, but their ionization is

253   significantly suppressed in FW and PW. In comparison, the additives that favor sodiated adducts

254    $[M+Na]^+$ in nanopure exhibit suppressed ionization in MW, HFF, and FW, but their ionization is

255 significantly enhanced in PW. We expected this latter observation considering the elevated sodium

256 concentrations in the PW samples (Figure ESI1). However, we found FW 5H to have the highest sodium

257 concentrations among all of the water samples, yet we did not observe enhanced ionization of additives

258 that favor sodiated adducts in the FW 5H sample. Additionally, we found no statistically significant

259 association between sodium concentration and the ratio of the peak areas of sodiated and protonated

260 adducts among additives that exhibited both types of adducts, suggesting that sodium concentration

261 was not predictive of shifting adduct formation. We therefore conclude that the enhanced ionization of

262 additives that favor sodiated adducts in the PW is not exclusively the result of increasing sodium

263 concentrations, but is rather related to other features of the matrix that remain unidentified.

264 **Mechanisms Contributing to MRFs.** Enhanced or suppressed ionization of HFF additives can be caused

265 by at least two mechanisms: changes in ionization efficiency resulting from co-eluting matrix

266 constituents or the shifting of adduct ratios across varying matrices.[16] To further examine the

267 mechanism behind the MRFs reported in **Figure 1**, we calculated the ratio of the peak areas of sodiated

268 and protonated adducts among additives that exhibited both types of adducts in spiked nanopure and

269 prepared water samples. These adducts were selected because they were the dominant adducts

270 detected for the majority of additives in the environmental matrices. We normalized the ratio of the

271 peak areas of sodiated and protonated adducts calculated in the prepared water samples to the ratio

272 calculated for the spiked nanopure. This normalization allowed for an examination of the enhancement

273 of adducts even if the sodiated adduct was already dominant in nanopure water. The results of this

274 analysis are provided in **Figure 2**. Of the ten additives that exhibited both sodiated and protonated

275 adducts, six exhibited a clear trend in the shift of the ratio of these adducts in the different matrices. The

276 remaining additives either did not exhibit any notable trend or had at least one adduct that was not

277 detected in all samples. Interestingly, all six of the additives that exhibited trends in adduct shifting also

278 exhibited enhanced ionization in the PW samples as shown in **Figure 1**. For 2-butoxyethanol, bis(2-

279   ethylhexyl) phthalate, butyl glycidyl ether, and a representative nonylphenol ethoxylate (NPE-EO7),

280   polyethylene glycol (PEG-EO9), and polypropylene glycol (PPG-PO6), the ratio of sodiated to protonated

281   adducts was the same in MW as in nanopure. However, the ratio shifted to favor the protonated

282   adducts in the HFF samples and to favor sodiated adducts in the PW samples. These observations

283   confirm that the enhanced ionization observed in the PW samples is the result of adduct shifting, though

284   it remains unclear why enhanced ionization by means of adduct shifting is only observed in PW samples

285   and not in the similarly saline FW samples.

286   We also sought to explore the mechanisms contributing to the measured MRFs across all

287   homologues in each of the homologous mixtures. In the case of ADBAC, we could only calculate a MRF

288   for ADBAC-C_{12} because it was the major component of the homologous mixture. For PEG, PPG, and

289   CAPHS, there was no statistically significant difference in the average MRF calculated for each member

290   of the homologous mixture (one-way ANOVA, p=0.90, p=0.26, p=0.49, respectively). For CAPDMA, there

291   were significant differences in the MRFs calculated among the homologues (one-way ANOVA, p=1.43E-

292   08), but there was no clear trend among the differences, so we cannot currently propose a mechanism

293   which explains these differences. Finally, there were also significant differences in the MRFs calculated

294   among the NPE homologues (one-way ANOVA, p=4.97E-04), and there was a significant negative

295   association between the magnitude of the MRF and the chain length of the homologue between NPE-

296   EO5 to EO10. Further analysis of the ratio of sodiated to protonated adducts normalized to the ratio in

297   nanopure water indicated that, as the ethoxylate chain length increased, the prevalence of sodium

298   adducts in the FW and PW was less pronounced. While we could not find literature supporting this

299   specific shift, this is in line with the shift towards protonated and ammoniated adducts observed in PEG

300   and PPG with longer ethoxylated chains.[14]

301   **Generalizing Matrix Recovery Factors across Sample Types.** We finally sought to explore whether the

302   MRFs measured among the HFF additives could be generalized across water samples, which would

303   enable extrapolation of MRFs to other water samples of similar types. The data in **Figure 3** summarize

304   the range of MRFs calculated among seventeen of the HFF additives (all except EDTA and

305   bis(hexamethylene) triamine and only one representative homologue among the compounds included in

306   homologous mixtures) in each of the water samples. The box plot presents the median MRF among the

307   seventeen HFF additives (solid line in box) along with the first and third quartiles and the minimum and

308   maximum values. The data reveal that the MW have median MRFs close to 1.0 with a relatively narrow

309   range and the MRFs for the MW are never greater than 1.0. This is consistent with the TDS and inorganic

310   cation measurements and the calculated MRFs for MW are within the ranges expected for surface

311   waters.[40] The calculated MRFs for FW samples also have a relatively narrow range and are generally less

312   than 1.0. In HFF and PW, at least 25% of the HFF additives in all samples exhibited either no change in

313   ionization or enhanced ionization relative to nanopure, demonstrating more complex relationships

314   between matrix chemistry and ionization potential in these water samples. When all sample types are

315   considered, there were statistically significant differences in the distributions of the MRFs among the

316   water samples (Friedman test, $p=0.002$). Specifically, we found statistically significant differences

317   between FW 5H and PW 3H from W1 (pairwise comparison, $p<0.001$), W2 (pairwise comparison,

318    $p=0.001$), and W3 (pairwise comparison, $p= 0.039$). Despite some variability in the MRFs calculated

319   among the PW samples, we did not find statistically significant differences among PWs sampled from

320   the same well at different times (all combinations, pairwise comparison, $p=1.0$) or between PW

321   sampled from different wells (all combinations, pairwise comparison, $p=1.0$). This suggests that MRFs

322   calculated for an HFF additive in any PW sample could be extrapolated to quantify that additive in any

323   other PW sample, though this is only exemplified among our PW samples and further research would be

324   required to see if this observation can be generalized to samples collected from other wells.

325   **Screening for HF Additives in Water Samples.** The FracFocus disclosures for MIP 3H and 5H are

326   provided in Tables ESI11 – ESI16. The disclosures include 40 unique chemical additives, with 33 of them

327   being organic chemicals and five of those being amenable to LC-ESI-MS analysis (glutaraldehyde, ADBAC,

328   PEG, PPG, and guar gum).[12] We first leveraged the high-resolution mass spectral acquisitions obtained

329   for each water sample to screen for the disclosed HF additives, the HF additives included in our

330   compound tuning and MRF experiments, and other priority HF additives and expected transformation

331   products using previously described techniques.[35] We detected four of the disclosed additives in at least

332   one of the water samples collected from MIP 3H or 5H: glutaraldehyde, and homologues of ADBAC, PEG,

333   and PPG. We did not detect guar gum, likely due to its ready biodegradability.[41] We also did not detect

334   2-acrylamido-2-methylpropanesulfonic acid, but it was not explicitly included in the HFF mixture; we

335   included it in the analysis because it was a suspected transformation product of disclosed polymers used

336   in the HFF.

337   Glutaraldehyde, one of the most commonly used biocides,[32,42] was disclosed in both wells, but

338   we detected it only in HFF from well 3H ([M+H]$^+$, RT 7.7 min, 1.82 ppm error). The absence of

339   glutaraldehyde in the wastewaters is consistent with previous findings and attributable to its tendency

340   to biodegrade and auto-polymerize.[13,43] Similar to what was reported in a previous study, we observed a

341   hydrated and sodiated adduct of a dimerized molecule of glutaraldehyde ([2M+H$_2$O+Na]$^+$, RT 10.4 min,

342   0.15 ppm error) in HFF 3H at an accurate mass (m/z) of 241.1048. The higher retention time indicates

343   that this polymer is a product of an aldol condensation reaction, and not an artifact formed in the

344   source.[13] We also observed a trimer ([3M+H$_2$O+Na]$^+$, RT 11.9 min, 0.28 ppm error), further complicating

345   our subsequent attempts of quantification. To properly quantify the total concentration of

346   glutaraldehyde polymers, it has been suggested that derivatization with 2,4-dinitrophenylhydrazine is

347   necessary.[16] Analytical data supporting these observations is provided in Figure ESI2.

348   We detected ADBAC, a commonly used antimicrobial surfactant,[32,42] as ADBAC-C$_{12}$ ([M]$^+$, RT 18.0

349   min, -0.35 ppm error), ADBAC-C$_{14}$ ([M]$^+$, RT 19.9 min, -0.26ppm error), and ADBAC-C$_{16}$ ([M]$^+$, RT 21.3 min,

350   -0.49 ppm error) in both HFF samples with accurate masses (m/z) of 304.2998, 332.3311, and 360.3623,

351   respectively. We also found ADBAC-C_{12} in all FW and PW samples, which will be discussed later with

352   respect to quantification in detail. Trace levels of other ADBAC homologues were also detected

353   sporadically among the water samples including the C_6, C_8, C_{10}, and C_{18} homologues. A Kendrick mass

354   analysis[14,15] supporting these observations is provided in Table ESI17.

355   We detected PEGs ranging from PEG-EO5 ([M+Na]$^+$, RT 8.4 min, 0.58 ppm error) to PEG-EO14

356   ([M+NH$_4$]$^+$, RT 10.2 min, 0.77 ppm error). In this analysis, PEG-EO5 was the only PEG homologue where

357   the sodiated adduct was dominant. For PEG-EO6 and the PEG homologues with longer ethoxylated

358   chains, the ammoniated adduct was dominant. This shift is consistent with previous studies which

359   detected PEG and PPG in FW and PW from other formations and noted a shift in adducts related to the

360   length of the ethoxylated and propylated chains.[14,15,37] Specifically, it was previously noted that PEG

361   homologues with an ethoxylate chain length of seven or fewer form predominantly sodiated adducts

362   and PEG homologues with an ethoxylate chain length of nine or greater form predominantly

363   ammoniated adducts.[14] A similar phenomenon was described for PPG, with sodiated adducts being

364   greater in intensity for PPG-PO6 and homologues with shorter propylated chains and ammoniated

365   adducts being greater in intensity for PPG-PO8 and homologues with greater propylated chain length.[15]

366   With respect to PPG, this study found PPG homologues ranging from PPG-PO4 ([M+Na]$^+$, RT 11.7 min, -

367   0.02 ppm error) to PPG-PO11 ([M+H]$^+$, RT 18.3 min, 1.13 ppm error). However, we found the sodiated

368   adducts for PPG homologues with greater intensity than the ammonium adduct, even for homologues

369   with chain lengths greater than that of PPG-PO8. Instead, protonated adducts were dominant for PPG-

370   PO8 and other homologues with greater propylated chain lengths. This phenomenon is similar to what

371   was previously reported, however, it suggests that the adducts formed in previous studies may not be

372   entirely due to structural changes promoting stronger complexation of ammonium as previously

373   hypothesized,[14,15] but may be at least partially due to the ammonium concentrations in the samples or

374   an instrument-specific phenomenon. Kendrick mass analyses supporting these observations are

375   provided in Tables ESI18 and ESI19.

376   Interestingly, despite the fact that it was not disclosed in the FracFocus report, we also

377   measured 2-butoxyethanol (2-BE, [M+Na]$^+$, RT 10.7 min, 0.773 ppm error) in all FW and PW samples. We

378   measured 2-BE with an accurate mass (m/z) of 141.0887, which matches the MS spectra acquired for 2-

379   BE using the analytical grade standard (see Table ESI9). We also confirmed MS/MS fragments with

380   accurate masses (m/z) of 57.0707 and 105.0035. Due to its absence from both the FracFocus disclosure

381   and the HFF samples, 2-BE was likely not used as a chemical additive in the process of well completion

382   and may be derived from another source, which has yet to be determined. 2-BE is commonly used as a

383   surfactant, corrosion inhibitor, and nonemulsifier and was found to be in 22.8% of FracFocus disclosures

384   in a 2015 review and may have been used as an additive (e.g., maintenance chemical) subsequent to the

385   fracturing of the wells.[32] It has previously been identified in FW and PW samples using 2D gas

386   chromatography coupled to time-of-flight mass spectrometry in FW and PW samples and groundwater

387   samples near drilling operations.[11] This is the first known measurement of 2-BE in HF affiliated fluids

388   using LC-ESI-MS, although targeted LC-ESI-MS methods have been developed for detection of 2-BE in

389   seawater because it was a component of dispersant formulations used to remediate the effects of the

390   Macondo well blowout.[44] Analytical data supporting these qualitative observations is provided in Figure

391   ESI3.

392   **Quantification of ADBACs.** We used the MRFs calculated for each additive to provide the first

393   quantitative estimates of multiple HFF additives using LC-ESI-MS. We performed quantification of

394   ADBAC-C$_{12}$ using calibration curves prepared from a pure standard and from a homologous mixture

395   containing ADBAC-C$_{12}$, ADBAC-C$_{14}$, and ADBAC-C$_{16}$. In the latter approach, we assumed that each

396   individual homologue was ionized with the same efficiency and assigned concentrations to each

397   homologue in each sample of the calibration curve based on the fraction of the total peak area each

17

398   homologue contained. The results of the quantification of ADBAC-C_{12} using both approaches is provided

399   in **Figure 4**, where error bars represent the uncertainty in the linearity of the respective calibration

400   curves. We quantified ADBAC-C_{12} in all samples, with concentrations found in the low mg·L^{-1} level in the

401   HFF and in the low μg·L^{-1} level in the MW, FW, and PW. The results also indicate that the quantitative

402   estimates for ADBAC-C_{12} were not significantly different when using calibration curves prepared from a

403   pure standard or from a homologous mixture. Despite greater uncertainty in the estimates made from

404   the calibration curve prepared from a homologous mixture, both approaches result in concentrations

405   within a factor of two (even when considering uncertainty) which is appropriate for most exposure

406   assessments.

407   Because the quantitative estimates of ADBAC-C_{12} were reasonable when using the calibration

408   curve prepared with a homologous mixture, we could extend our analysis to quantify ADBAC-C_{14} and

409   ADBAC-C_{16} in the HFF with the total peak area approach.[45] We found both of these homologues at the

410   low mg·L^{-1} level in both HFF samples, resulting in total ADBAC concentrations of 3.59 mg·L^{-1} for HFF 3H

411   and 8.01 mg·L^{-1} in HFF 5H. These findings are consistent with the FracFocus report, which indicated that

412   approximately 7 mg·L^{-1} level of total ADBAC-C_{12} to C_{16} was present in the HFF. It is notable that we

413   measured significant levels of ADBAC-C_{14} and ADBAC-C_{16} in the HFF but not in any of the wastewater

414   samples. This suggests that ADBAC may be transformed in the subsurface, likely through mechanisms of

415   chain shortening to form ADBAC homologues of shorter chain length or by cleavage of the alkyl group to

416   form benzyl dimethyl amine.[46] We found qualitative evidence of ADBAC homologues of shorter chain

417   length in the FW and PW samples, though our homologous mixture did not contain those homologues

418   so we could not quantify them.

419   **Quantification of PEGs and PPGs.** We used the same total peak area approach that we validated with

420   ADBAC to quantify PEGs and PPGs in the prepared water samples. For quantification, we only

421   considered homologues that made up greater than 5% of the homologous mixture and that were

422 detected with peak intensities at least twice as high as those found in filtered nanopure blanks. These

423 selection criteria limited quantification to PEG-EO10 through PEG-EO14 and to PPG-PO5 through PPG-

424 PO8. The results of the quantifications are provided in **Figure 5**. Notably, while both PEG and PPG were

425 detected in FWs and PWs, PPG was not detected in MWs or HFFs and PEG was not detected in MWs or

426 HFF 3H. PEG-EO10 to PEG-EO14 homologues were detected in HFF 5H with a total concentration of 60.2

427 $\mu g \cdot L^{-1}$. We note two important trends for both groups of homologues. First, total PEG and PPG

428 concentrations (within the range of homologues quantified) are greatest in FW samples and decrease in

429 PW samples. Total PEG concentrations were on the order of 100 $\mu g \cdot L^{-1}$ in FW samples and ranged down

430 to 4.2 $\mu g \cdot L^{-1}$ in week 2 PW samples before dropping below our LODs. We found total PPG concentrations

431 in a similar range, and PPG-PO5 remained above our LOD in all PW samples. These measured

432 concentrations are much lower than previous semi-quantitative estimates of total PEG and PPG

433 concentrations in HFF wastewaters.[15] The discrepancy can be explained at least in part due to the

434 enhanced ionization of PEGs and PPGs we observed in PW samples resulting in MRFs greater than 1.0;

435 this results in a downward adjustment in estimated concentrations that has not been accounted for in

436 previous studies. Further, our quantification includes only a limited range of PEG and PPG homologues

437 that were present in our homologous mixtures. Like ADBAC, we expect that greater concentrations of

438 shorter chain homologues may be present which would result in higher total concentrations of PEG and

439 PPG. Second, there is a negative association between concentration and chain length of each

440 homologue. In other words, shorter chain homologues are present at greater concentrations, suggesting

441 degradation of longer chain PEGs and PPGs or other alcohol ethoxylates into shorter chain

442 homologues.[47] Further work that quantifies additional short chain homologues and evaluates changes in

443 the concentrations of homologues of varying chain length to better assess transformation is warranted.

444 **CONCLUSIONS**

445 This research addresses two important knowledge gaps related to the measurement of polar to semi-

446 polar chemical additives in HF-associated fluids. First, we report MS and MS/MS acquisition parameters

447 for nineteen priority HF additives and quantify the ways in which seventeen of these additives'

448 ionization is enhanced or suppressed in water samples collected over the life cycle of a HF gas well with

449 MRFs. These data clearly demonstrate that the changing matrix of water samples from MW through PW

450 can have changing effects on the ionization of chemical additives. It is notable that most compounds

451 have suppressed ionization in most types of samples, though additives that form sodiated adducts in

452 nanopure water have enhanced ionization in PW samples. These include some of the most widely

453 reported HF additives including glutaraldehyde, NPEs, PEGs, PPGs, whose concentrations in PW can be

454 overestimated if enhanced ionization is not considered in their analysis. Through further analysis, we

455 demonstrate that enhanced ionization is most likely the result of adduct shifting and we expect this to

456 be generalized across PW samples, perhaps even from wells in different formations. Second, we provide

457 the first quantitative estimates of individual homologues of ADBAC, PEG, and PPG in HF-associated

458 fluids. Notably, our estimates of ADBAC concentrations agree with what was reported in the FracFocus

459 disclosure, adding some additional validation to our approach and providing some evidence of the

460 accuracy of data in FracFocus disclosures. In the case of ethoxylated homologous mixtures, we found

461 increasing concentrations of shorter chain homologues in later wastewater samples, also providing

462 evidence of transformation, likely by the mechanism of chain shortening. Together, these data provide

463 the first quantitative measurements that can be used to inform future toxicity studies or exposure

464 assessments.

465 **ACKNOWLEDGEMENTS**

472 **CITATIONS**

473 1   J. Perrin, T. Cook and (US Energy Information Administration), Hydraulically fractured wells

474   provide two-thirds of U.S. natural gas production,

475   https://www.eia.gov/todayinenergy/detail.php?id=26112, (accessed 8 June 2017).

476 2   K. Dyl, V. Zaretskaya and (US Energy Information Administration), In new trend, U.S. natural gas

477   exports exceeded imports in 3 of the first 5 months of 2017,

478   https://www.eia.gov/todayinenergy/detail.php?id=32392, (accessed 8 August 2017).

479 3   M. Bamberger and R. E. Oswald, Unconventional oil and gas extraction and animal health,

480   *Environ. Sci. Process. Impacts*, 2014, **16**, 1860–1865.

481 4   E. G. Elliott, A. S. Ettinger, B. P. Leaderer, M. B. Bracken and N. C. Deziel, A systematic evaluation

482   of chemicals in hydraulic-fracturing fluids and wastewater for reproductive and developmental

483   toxicity, *J. Expo. Sci. Environ. Epidemiol.*, 2017, **27**, 90–99.

484 5   B. G. Rahm, J. T. Bates, L. R. Bertoia, A. E. Galford, D. A. Yoxtheimer and S. J. Riha, Wastewater

485   management and Marcellus Shale gas development: Trends, drivers, and planning implications, *J.*

486   *Environ. Manage.*, 2013, **120**, 105–113.

487 6   L. O. Haluszczak, A. W. Rose and L. R. Kump, Geochemical evaluation of flowback brine from

488   Marcellus gas wells in Pennsylvania, USA, *Appl. Geochemistry*, 2013, **28**, 55–61.

489 7   US Environmental Protection Agency - US EPA, *Hydraulic Fracturing for Oil and Gas: Impacts from*

490   *the Hydraulic Fracturing Water Cycle on Drinking Water Resources in the United States (Main*

491   *Report - EPA/600/R-16/236fa)*, 2016.

492 8   T. Colborn, C. Kwiatkowski, K. Schultz, M. Bachran, C. Taylor, T. Colborn, C. Kwiatkowski, K.

493   Schultz and M. Bachran, Natural Gas Operations from a Public Health Perspective, *Hum. Ecol. Risk*

494   *Assess. An Int. J.*, 2011, **17**, 1–25.

495 9   B. D. Drollette, K. Hoelzer, N. R. Warner, T. H. Darrah, O. Karatum, M. P. O'Connor, R. K. Nelson,

496   L. A. Fernandez, C. M. Reddy, A. Vengosh, R. B. Jackson, M. Elsner and D. L. Plata, Elevated levels

497   of diesel range organic compounds in groundwater near Marcellus gas operations are derived

498   from surface activities, *Proc. Natl. Acad. Sci.*, 2015, **112**, 13184–13189.

499   10   W. Orem, C. Tatu, M. Varonka, H. Lerch, A. Bates, M. Engle, L. Crosby and J. McIntosh, Organic

500   substances in produced and formation water from unconventional natural gas extraction in coal

501   and shale, *Int. J. Coal Geol.*, 2014, **126**, 20–31.

502   11   G. T. Llewellyn, F. Dorman, J. L. Westland, D. Yoxtheimer, P. Grieve, T. Sowers, E. Humston-

503   Fulmer and S. L. Brantley, Evaluating a groundwater supply contamination incident attributed to

504   Marcellus Shale gas development, *Proc. Natl. Acad. Sci.*, 2015, **112**, 6325–6330.

505   12   G. J. Getzinger, M. P. O'Connor, K. Hoelzer, B. D. Drollette, O. Karatum, M. A. Deshusses, P. L.

506   Ferguson, M. Elsner and D. L. Plata, Natural Gas Residual Fluids: Sources, Endpoints, and Organic

507   Chemical Composition after Centralized Waste Treatment in Pennsylvania, *Environ. Sci. Technol.*,

508   2015, **49**, 8347–8355.

509   13   I. Ferrer and E. M. Thurman, Analysis of hydraulic fracturing additives by LC/Q-TOF-MS, *Anal.*

510   *Bioanal. Chem.*, 2015, **407**, 6417–6428.

511   14   E. M. Thurman, I. Ferrer, J. Blotevogel and T. Borch, Analysis of Hydraulic Fracturing Flowback and

512   Produced Waters Using Accurate Mass: Identification of Ethoxylated Surfactants, *Anal. Chem.*,

513   2014, **86**, 9653–9661.

514   15   E. M. Thurman, I. Ferrer, J. Rosenblum, K. Linden and J. N. Ryan, Identification of Polypropylene

515   Glycols and Polyethylene Glycol Carboxylates in Flowback and Produced Water from Hydraulic

516   Fracturing, *J. Hazard. Mater.*, 2017, **323**, 11–17.

517   16   K. Oetjen, C. G. S. Giddings, M. McLaughlin, M. Nell, J. Blotevogel, D. E. Helbling, D. Mueller and

518   C. P. Higgins, Emerging analytical methods for the characterization and quantification of organic

519   contaminants in flowback and produced water, *Trends Environ. Anal. Chem.*, 2017, **15**, 12–23.

520 17 Y. He, S. L. Flynn, E. J. Folkerts, Y. Zhang, D. Ruan, D. S. Alessi, J. W. Martin and G. G. Goss,

521 Chemical and toxicological characterizations of hydraulic fracturing flowback and produced

522 water, *Water Res.*, 2017, **114**, 78–87.

523 18 P. F. Ziemkiewicz and Y. Thomas He, Evolution of water chemistry during Marcellus Shale gas

524 development: A case study in West Virginia, *Chemosphere*, 2015, **134**, 224–231.

525 19 K. L. Rundlett and D. W. Armstrong, Mechanism of signal suppression by anionic surfactants in

526 capillary electrophoresis - electrospray ionization mass spectrometry, *Anal. Chem.*, 1996, **68**,

527 3493–3497.

528 20 N. B. Cech and C. G. Enke, Practical implications of some recent studies in electrospray ionization

529 fundamentals, *Mass Spectrom. Rev.*, 2001, **20**, 362–387.

530 21 K. Tang and R. D. Smith, Physical/chemical separations in the break-up of highly charged droplets

531 from electrosprays, *J. Am. Soc. Mass Spectrom.*, 2001, **12**, 343–347.

532 22 M. Thompson and S. L. R. Ellison, A review of interference effects and their correction in chemical

533 analysis with special reference to uncertainty, *Accredit. Qual. Assur.*, 2005, **10**, 82–97.

534 23 M. Stüber and T. Reemtsma, Evaluation of three calibration methods to compensate matrix

535 effects in environmental analysis with LC-ESI-MS, *Anal. Bioanal. Chem.*, 2004, **378**, 910–916.

536 24 C. R. Mallet, Z. Lu and J. R. Mazzeo, A study of ion suppression effects in electrospray ionization

537 from mobile phase additives and solid-phase extracts, *Rapid Commun. Mass Spectrom.*, 2004, **18**,

538 49–58.

539 25 E. Stokvis, H. Rosing and J. H. Beijnen, Stable isotopically labeled internal standards in

540 quantitative bioanalysis using liquid chromatography/mass spectrometry: necessity or not?,

541 *Rapid Commun. Mass Spectrom.*, 2005, **19**, 401–407.

542 26 G. Fedorova, T. Randak, R. H. Lindberg and R. Grabic, Comparison of the quantitative

543 performance of a Q-Exactive high-resolution mass spectrometer with that of a triple quadrupole

544   tandem mass spectrometer for the analysis of illicit drugs in wastewater, *Rapid Commun. Mass*

545   *Spectrom.*, 2013, **27**, 1751–1762.

546   27   D. E. Helbling, D. R. Johnson, M. Honti and K. Fenner, Micropollutant Biotransformation Kinetics

547   Associate with WWTP Process Parameters and Microbial Community Characteristics, *Environ. Sci.*

548   *Technol.*, 2012, **46**, 10579–10588.

549   28   H. Trufelli, P. Palma, G. Famiglini and A. Cappiello, An overview of matrix effects in liquid

550   chromatography-mass spectrometry, *Mass Spectrom. Rev.*, 2011, **30**, 491–509.

551   29   E. Barbot, N. S. Vidic, K. B. Gregory and R. D. Vidic, Spatial and temporal correlation of water

552   quality parameters of produced waters from Devonian-age shale following hydraulic fracturing,

553   *Environ. Sci. Technol.*, 2013, **47**, 2562–2569.

554   30   K. Oetjen, K. E. Chan, K. Gulmark, J. H. Christensen, J. Blotevogel, T. Borch, J. R. Spear, T. Y. Cath

555   and C. P. Higgins, Temporal characterization and statistical analysis of flowback and produced

556   waters and their potential for reuse, *Sci. Total Environ.*, 2018, **619–620**, 654–664.

557   31   C. Díez, M. Feinberg, A. S. Spörri, E. Cognard, D. Ortelli, P. Edder and S. Rudaz, Evaluation of

558   Quantification Methods to Compensate for Matrix Effects in the Analysis of Benzalkonium

559   Chloride and Didecyldimethylammonium Chloride in Fruits and Vegetables by LC-ESI-MS/MS,

560   *Food Anal. Methods*, 2016, **9**, 485–499.

561   32   J. D. Rogers, T. L. Burke, S. G. Osborn and J. N. Ryan, A Framework for Identifying Organic

562   Compounds of Concern in Hydraulic Fracturing Fluids Based on Their Mobility and Persistence in

563   Groundwater, *Environ. Sci. Technol. Lett.*, 2015, **2**, 158–164.

564   33   J. L. Luek, M. Harir, P. Schmitt-Kopplin, P. J. Mouser and M. Gonsior, Temporal dynamics of

565   halogenated organic compounds in Marcellus Shale flowback, *Water Res.*, 2018, **136**, 200–206.

566   34   C. M. G. Carpenter and D. E. Helbling, Removal of micropollutants in biofilters: Hydrodynamic

567   effects on biofilm assembly and functioning, *Water Res.*, 2017, **120**, 211–221.

568 35 A. L. Pochodylo and D. E. Helbling, Emerging investigators series: prioritization of suspect hits in a

569   sensitive suspect screening workflow for comprehensive micropollutant characterization in

570   environmental samples, *Environ. Sci. Water Res. Technol.*, 2017, **3**, 54–65.

571 36 S. J. Maguire-Boyle and A. R. Barron, Organic compounds in produced waters from shale gas

572   wells, *Environ. Sci. Process. Impacts*, 2014, **16**, 2237–2248.

573 37 J. Rosenblum, E. M. Thurman, I. Ferrer, G. Aiken and K. G. Linden, Organic Chemical

574   Characterization and Mass Balance of a Hydraulically Fractured Well: From Fracturing Fluid to

575   Produced Water over 405 Days, *Environ. Sci. Technol.*, 2017, **51**, 14006–14015.

576 38 P. L. Ferguson, C. R. Iden and B. J. Brownawell, Analysis of Alkylphenol Ethoxylate Metabolites in

577   the Aquatic Environment Using Liquid Chromatography–Electrospray Mass Spectrometry, *Anal.*

578   *Chem.*, 2000, **72**, 4322–4330.

579 39 P. A. Lara-Martín, E. González-Mazo and B. J. Brownawell, Multi-residue method for the analysis

580   of synthetic surfactants and their degradation metabolites in aquatic systems by liquid

581   chromatography–time-of-flight-mass spectrometry, *J. Chromatogr. A*, 2011, **1218**, 4799–4807.

582 40 V. Leendert, H. Van Langenhove and K. Demeestere, Trends in liquid chromatography coupled to

583   high-resolution mass spectrometry for multi-residue analysis of organic micropollutants in

584   aquatic environments, *TrAC Trends Anal. Chem.*, 2015, **67**, 192–208.

585 41 Y. Lester, T. Yacob, I. Morrissey and K. G. Linden, Can We Treat Hydraulic Fracturing Flowback

586   with a Conventional Biological Process? The Case of Guar Gum, *Environ. Sci. Technol. Lett.*, 2014,

587   **1**, 133–136.

588 42 M. Elsner and K. Hoelzer, Quantitative Survey and Structural Classification of Hydraulic Fracturing

589   Chemicals Reported in Unconventional Gas Production, *Environ. Sci. Technol.*, 2016, **50**, 3290–

590   3314.

591 43 G. A. Kahrilas, J. Blotevogel, E. R. Corrin and T. Borch, Downhole Transformation of the Hydraulic

592   Fracturing Fluid Biocide Glutaraldehyde: Implications for Flowback and Produced Water Quality,

593   *Environ. Sci. Technol.*, 2016, **50**, 11414–11423.

594   44   C. E. Ramirez, S. R. Batchu and P. R. Gardinali, High sensitivity liquid chromatography tandem

595   mass spectrometric methods for the analysis of dioctyl sulfosuccinate in different stages of an oil

596   spill response monitoring effort, *Anal. Bioanal. Chem.*, 2013, **405**, 4167–4175.

597   45   I. Ferrer and E. T. Furlong, Identification of Alkyl Dimethylbenzylammonium Surfactants in Water

598   Samples by Solid-Phase Extraction Followed by Ion Trap LC/MS and LC/MS/MS, *Environ. Sci.*

599   *Technol.*, 2001, **35**, 2583–2588.

600   46   G. A. Kahrilas, J. Blotevogel, P. S. Stewart and T. Borch, Biocides in Hydraulic Fracturing Fluids: A

601   Critical Review of Their Usage, Mobility, Degradation, and Toxicity, *Environ. Sci. Technol.*, 2015,

602   **49**, 16–32.

603   47   K. M. Heyob, J. Blotevogel, M. Brooker, M. V. Evans, J. J. Lenhart, J. Wright, R. Lamendella, T.

604   Borch and P. J. Mouser, Natural Attenuation of Nonionic Surfactants Used in Hydraulic Fracturing

605   Fluids: Degradation Rates, Pathways, and Mechanisms, *Environ. Sci. Technol.*, 2017, **51**, 13985–

606   13994.
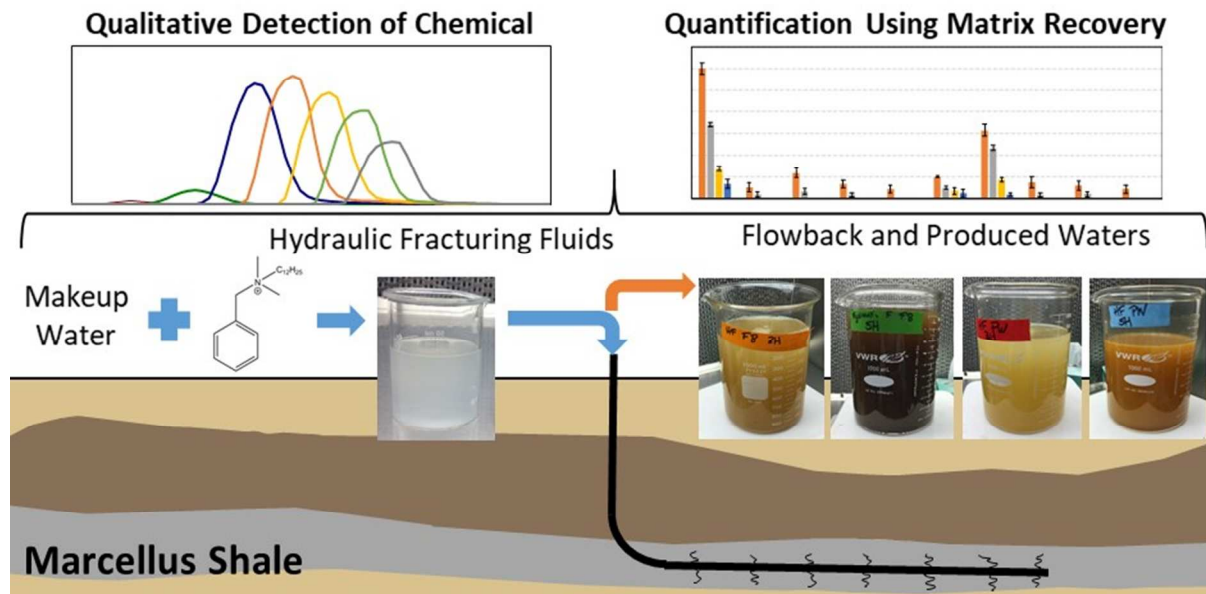
607

644

645   **TABLE OF CONTENTS ENTRY:** Liquid chromatography electrospray ionization mass spectrometry was

646   used to quantify chemical additives in water collected from unconventional shale gas wells.

647

648   **Graphical Abstract:**

649

	ADBAC-C12	CAPHS-C7H15	Didecyldimethylammonium chloride	Diethanolamine	CAPDMA-C7H15	NPE-EO37	2-acrylamidopropyl-2-methanesulfonic acid	Glutaraldehyde	NPE-EO7	Bis-(2-ethylhexyl) phthalate	2-butoxyethanol	Butyl Glycidyl Ether	PEG-EO9	PPG-PO6
	M+	M+	M+	M+H	M+H	M+2H	M-H	M+Na	M+Na	M+Na	M+Na	M+Na	M+Na	M+Na
MW 3H	0.89	0.94	0.46	0.97	0.95	0.88	0.96	0.73	0.63	1.00	0.67	0.84	0.67	0.83
MW 5H	0.66	0.91	0.29	0.95	0.99	0.67	0.96	0.88	0.56	0.92	0.72	0.85	0.74	0.85
HFF 3H	1.65	1.20	0.27	1.01	1.03	1.00	0.81	0.19	0.38	0.34	0.28	0.24	0.27	0.33
HFF 5H	1.49	1.20	0.18	0.94	1.02	1.39	0.86	0.48	0.67	0.38	0.51	0.43	0.49	0.55
FW 3H	0.72	0.71	0.25	0.20	0.74	0.54	0.13	0.49	0.53	1.04	0.85	0.98	0.44	0.76
FW 5H	0.86	0.41	0.21	0.06	0.43	0.25	0.39	0.99	0.47	0.56	0.32	0.61	-0.06	0.30
PW 3H Week 1	0.87	0.42	0.60	0.16	0.62	0.57	0.66	2.58	1.30	2.51	1.44	1.32	1.36	1.57
PW 3H Week 2	1.04	0.39	0.39	0.14	0.84	0.36	0.59	2.62	0.94	2.84	1.69	1.99	1.39	1.68
PW 3H Week 3	0.96	0.38	0.29	0.15	0.79	0.38	0.63	2.44	0.95	1.80	1.35	1.66	1.25	1.24
PW 3H Week 4	0.98	0.37	0.21	0.14	0.84	0.34	0.59	2.56	0.86	2.08	1.34	1.67	1.12	1.37
PW 5H Week 1	0.89	0.40	0.44	0.17	0.78	0.36	0.72	2.34	0.82	1.77	1.09	1.57	1.28	0.59
PW 5H Week 2	0.96	0.43	0.19	0.15	0.63	0.29	0.64	2.13	0.97	2.12	1.33	0.96	1.51	1.29
PW 5H Week 3	0.84	0.38	0.19	0.15	0.67	0.38	0.65	2.29	0.95	2.12	1.28	1.30	1.42	1.29
PW 5H Week 4	0.86	0.41	0.20	0.16	0.73	0.34	0.65	2.25	0.85	2.33	1.38	1.30	1.40	1.38

Figure 1. MRFs for fourteen of the selected compounds in each of the prepared water samples. MRFs in blue indicate enhancement and MRFs in red indicate suppression. MW is makeup water; HFF is hydraulic fracturing fluid; FW is flowback water; PW is produced water.

1
2
3
4
5
6
7
8
9
10
11
12
13
14
15
16
17
18
19
20
21
22
23
24
25
26
27
28
29
30
31
32
33
34
35
36
37
38
39
40
41
42
43
44
45
46
47
48
49
50
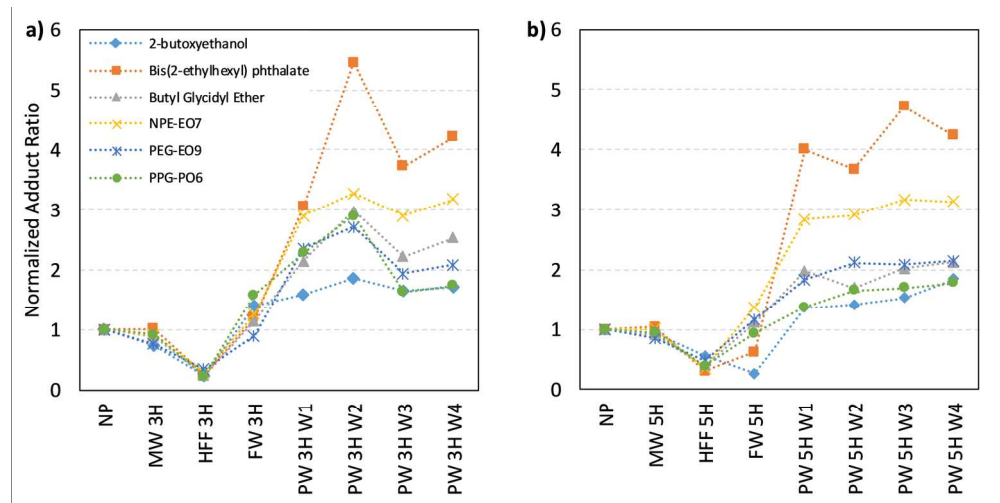51
52
53
54
55
56
57
58
59
60

Figure 2. The ratio of sodiated adduct peak area to protonated adduct peak area for each chemical in each sample, normalized to the same ratio in spiked nanopure water. Any values greater than one indicate a shift favoring sodiated adducts, whereas any values lower than one indicate a shift favoring protonated adducts. NP is nanopure water; MW is makeup water; HFF is hydraulic fracturing fluid; FW is flowback water; PW is produced water.

84x42mm (600 x 600 DPI)

1
2
3
4
5
6
7
8
9
10
11
12
13
14
15
16
17
18
19
20
21
22
23
24
25
26
27
28
29
30
31
32
33
34
35
36
37
38
39
40
41
42
43
44
45
46
47
48
49
50
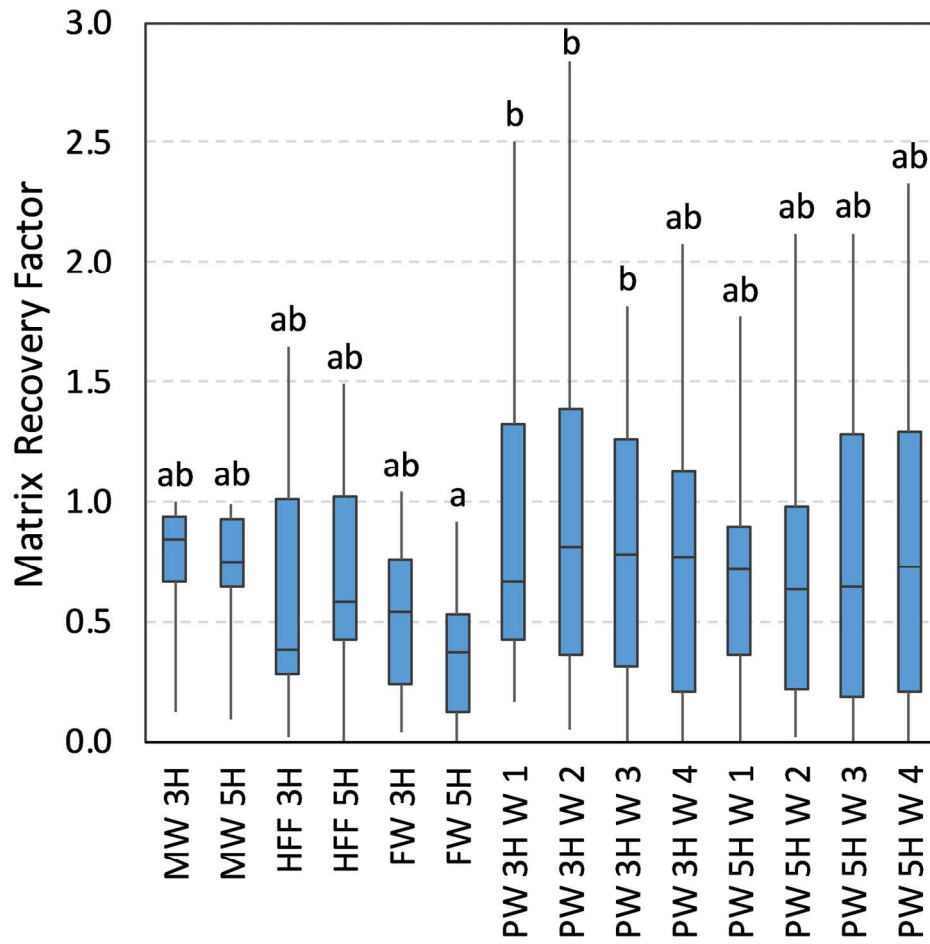51
52
53
54
55
56
57
58
59
60

Figure 3. Matrix recovery factors (MRFs) for HFF additives across makeup water (MW), hydraulic fracturing fluid (HFF), flowback water (FW) and produced water (PW). MW, FW, and PW were diluted 1:10 and HFF was diluted 1:100 prior to analysis. Boxes represent the distribution of MRFs for each of the seventeen additives that were successfully detected in each of the fluids. The line in the box represents the median MRF, the edges of the boxes represent the first and third quartile, the ends of the whiskers represent the minimum and maximum MRFs. Samples labeled with the same letter were not found to have statistically significant differences in distribution using a Friedman test followed by pairwise comparisons with Bonferroni corrections for multiple comparisons.
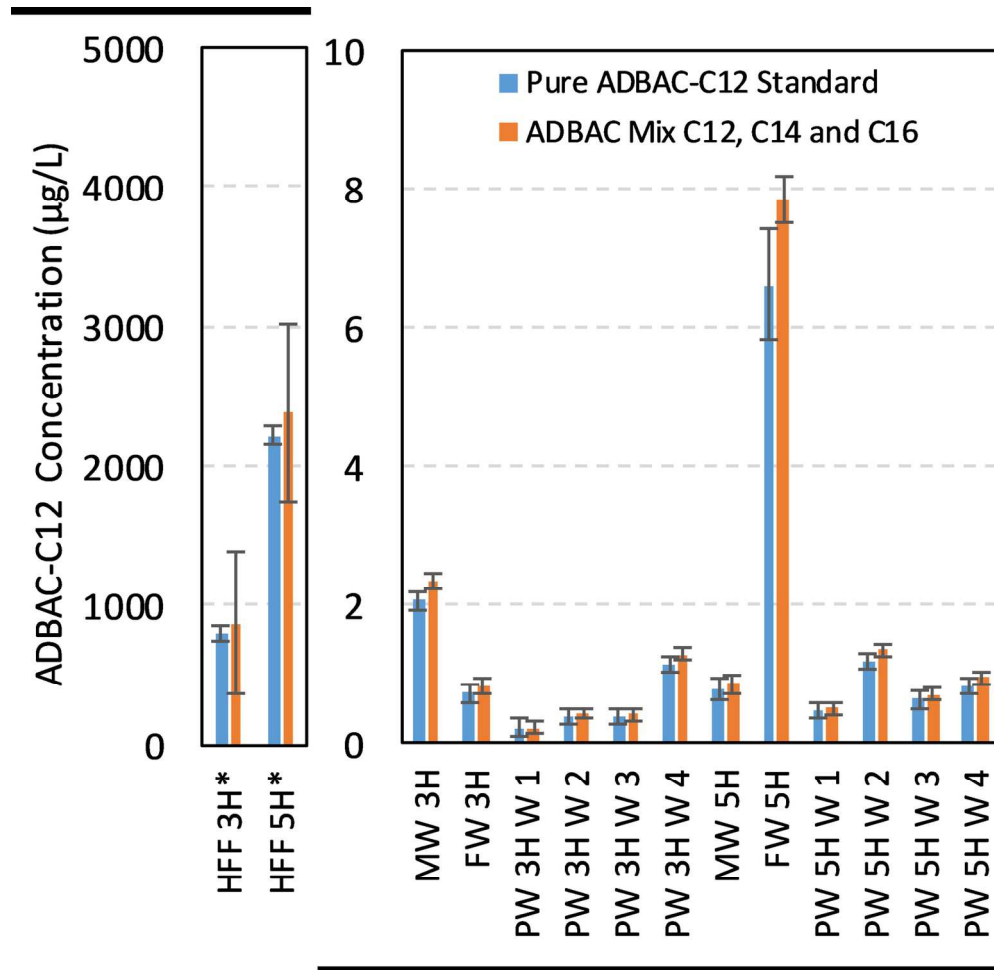
82x80mm (600 x 600 DPI)

1
2
3
4
5
6
7
8
9
10
11
12
13
14
15
16
17
18
19
20
21
22
23
24
25
26
27
28
29
30
31
32
33
34
35
36
37

Figure 4. Concentrations of ADBAC-C_{12} calculated using a calibration curve prepared using a pure analytical grade standard and a standard mix of three ADBAC homologues. The left panel has a concentration range of 0 – 4000 $\mu g \cdot L^{-1}$ for the y-axis and the right panel has a concentration of 0 – 10 $\mu g \cdot L^{-1}$ for the y-axis. *The MRFs for both HFF samples were determined using aliquots that were diluted by a factor of 100, which is 10 times more than the aliquots used for this quantification. This is a conservative estimate because we would expect the matrix effects to be less pronounced in more dilute aliquots. MW is makeup water; HFF is hydraulic fracturing fluid; FW is flowback water; PW is produced water.

79x77mm (600 x 600 DPI)

38
39
40
41
42
43
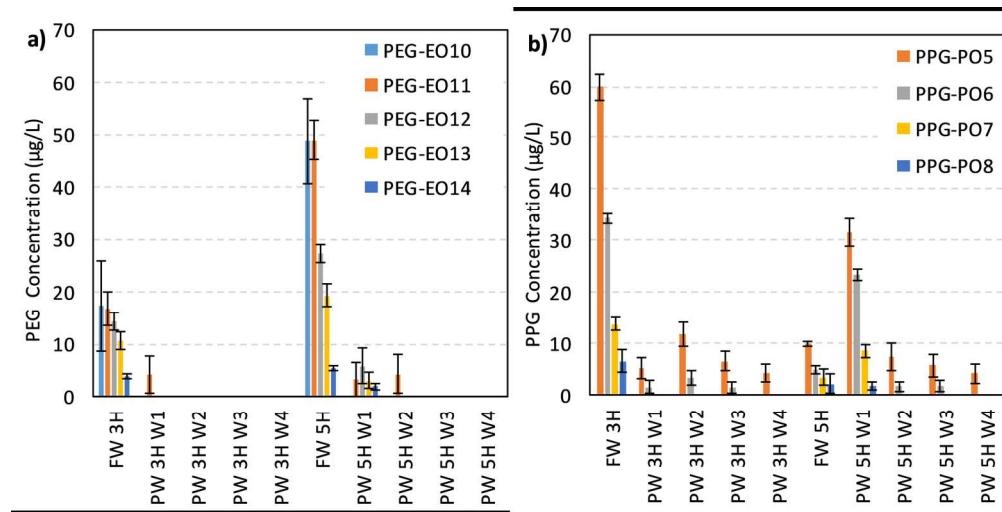44
45
46
47
48
49
50
51
52
53
54
55
56
57
58
59
60

Figure 5. Concentrations of PEG and PPG quantified using homologous mixtures. PPG was not detected in MWs or HFFs. PEG was not detected in MWs or HFF 3H, but was PEG-EO10 to PEG-EO14 homologues were detected in HFF 5H with a total concentration of 60.2 μg·L^{-1}. FW is flowback water; PW is produced water.

83x42mm (600 x 600 DPI)